A new Setup for probing condensed matter in the Far IR to THz ranges at sub-Kelvin temperatures on the AILES beamline at SOLEIL

Benjamin Langerome, Thomas Souske, Kelly Rader, Marine Verseils, Tongtong Lyu, Sophie de Brion, Laurent Manceron, Jean-Blaise Brubach, Pascale Roy

A new Setup for probing condensed matter in the Far IR to THz ranges at sub-Kelvin temperatures on the AILES beamline at SOLEIL

Benjamin Langerome[a], Thomas Souske[a], Kelly Rader[a], Marine Verseils[a], Lyu Tongtong[a], Sophie de Brion[b], Laurent Manceron[a,c], Jean-Blaise Brubach[a] and Pascale Roy[a]*

[a]AILES Beamline, Synchrotron SOLEIL, Gif-sur-Yvette Cedex, 91190, France

[b]Institut Néel, Université Grenoble Alpes, 38000, France

[c]MONARIS, UMR 8233, CNRS - Sorbonne Université, 4 place Jussieu, F-75005 Paris, France

Correspondence email: pascale.roy@synchrotron-soleil.fr

Funding information: ANR Dymage and Synchrotron SOLEIL.

Synopsis A new spectroscopic setup for sub-K solid state measurements at the open user facility AILES @SOLEIL is described. An example of a measurement of transmission and reflection in the 10 to 600 cm^{-1} range is presented..

Abstract We describe a spectroscopic setup dedicated to the optical study of materials in the sub-Kelvin temperature range, available on the AILES beamline of synchrotron SOLEIL. This ensemble, based on an adiabatic demagnetization refrigerator, has been designed for spectroscopy in the far-infrared and terahertz domain. The combination of the cryogenic set-up with synchrotron radiation allows for reflectivity and transmission measurements down to 95 mK and 144 mK, respectively, with reproducibility better than 0.5 %.

Keywords IR and THz spectroscopies; synchrotron radiation; sub-Kelvin temperatures; adiabatic demagnetization refrigeration;

1. Introduction

For studying condensed matter, the fine control of physical parameters such as temperature or pressure allows to explore different structures of a phase diagram or to verify some theoretical models. When this control is extended towards sub-Kelvin temperatures, remarkable quantum effects can occur in materials, such as transitions to superconducting states or the appearance of a quantum magnetic ordering. In these two cases, the low energy involved makes infrared (IR) and terahertz (THz) spectroscopies well suited to probe these excitations [1, 2]. The control of the temperature is also important to characterize the optical properties of detectors having an interest for astronomical applications [3-5]. Indeed, in many space missions, the detector must be cooled down to sub-Kelvin temperature in order to reduce significantly the thermal noise, essential to study the universe background radiation or low intensity THz sources.

To reach this sub-Kelvin temperature range on a material, two methods are commonly employed: dilution of ^{3}He in ^{4}He [3-5] or adiabatic demagnetization refrigerators (ADR) using paramagnetic salts [6,7]. For condensed matter studies developed on the AILES Beamline of Synchrotron SOLEIL (an open access facility [8]) the samples are usually in the mm^3 scale due to the complex chemical or physical syntheses. Thus, for the present development, the latter, ADR technology has been chosen, as it presents several crucial advantages in terms of size, operation costs and simplicity of operation. The adiabatic demagnetization refrigeration uses a magnetic cycle to cool down samples at temperatures as low as 50 mK. However, this technique does not provide continuous cooling power and this technology is limited to systems with relatively modest heat loads. It is therefore essential to design the system with stringent requirements regarding the heat loads created by the optical access. Another crucial point for spectroscopic measurements is the necessity of alleviating the thermal contraction effects to maintain precise alignments for small samples over the whole temperature range.

In order to couple a commercial ADR instrument to a spectrophotometer, an important development is thus needed, including the implementation of optical apertures to permit the light beam to probe the sample. As a consequence, this modification may degrade dramatically the cryogenic performances due to the heat load coming from the ambient background and/or from the source of probe radiation. This effect can be strongly limited by using the synchrotron radiation. Indeed, the source provided by AILES beamline is characterized by a high brilliance in the THz and FIR spectral ranges [8], as well as a small divergence, allowing a minimal source optical *étendue*. This paper is devoted to the description of the setup and a short example illustrates its present performances.

2. Requirements.

The adaptation of this sub-Kelvin cryostat to optical measurements requires modifications at three levels: mechanical, optical and cryogenic. These developments are interdependent and have been considered simultaneously. The main specifications are described below:

1) The sample must be able to reach temperatures down to 200 mK for a time sufficient to record the required spectra, with a temperature varying no more than 5%.

2) The vacuum must be sufficient to limit condensation of ice or atmospheric species on the sample. A vacuum of 10^{-6} mbar or less is required before starting the cooling, which then allows cryo-pumping on the cryogenerator upper parts.

3) The spectral range of the light reaching the sample has to be adjustable and filtered to the region of interest for the spectroscopic study. For the phenomena targeted in condensed matter, most of the excitations occurring at sub-Kelvin temperatures are expected in the THz or FIR range, defined arbitrary here as 0 – 100 cm^{-1} and 0 – 600 cm^{-1}, respectively.

4) The beam focal point must be at most 2 mm diameter at the sample plane with a cone opening of about 30°.

5) Two different optical configurations are required, to perform either reflectivity measurements on metallic samples or transmission measurements on transparent materials. Also, aligning *in situ* the optical beam with either visible part of the SR beam or an external light source using a camera should be possible.

3. Mechanical components

3.1. Description of the cryogenic system

The cryogenic ensemble, a cryogenerator Model 103 Rainier, from High Precision Devices (Boulder, USA) is coupled to the AILES Bruker IFS125HR Michelson interferometer. Its cooling cycle can be summarized as follows. As a first step, a precooling from 300 K to 3 K is carried out using a pulse tube helium cryostat. This cryostat is composed of a pulse-tube refrigerator cooling a 3 K stage. Once the system is stable at 3 K, the adiabatic demagnetization cycle applied to paramagnetic salts allows the temperature to go down from 3 K to sub-Kelvin temperatures. On this stage, two paramagnetic salts pills are fixed inside a magnetic shield: ferric aluminium alum (FAA) and gadolinium gallium garnet (GGG). The adiabatic demagnetization cycle is triggered by a surrounding superconducting coil. Gold-plated copper rods are attached to each of the salt pills and constitute the cold points of the cryostat. Two low temperature sensors ruthenium oxide (Scientific Inst.,W. Palm Springs, USA), provided with the ADR system and originally placed near the salt pills, have been lowered to the nearest possible points next to the clamp for the cold optics and sample holders. Their estimated accuracies are +/- 5mK. A third, calibrated sensor was added on the sample holder itself (see figures below).

The rod linked to GGG is cooled down to ~ 470 mK, while the one linked to FAA is cooled down to about 60 mK, without any optical port through the radiation shields. Cooling from room to about 3K takes 15 hours. Next, the magnetic cycle includes 45 minutes ramping up the magnetic field, 2 hours soak time at maximum field, followed by 45 minutes demagnetization. Overall, about 20 hours are necessary to achieve the minimal temperature on the cold tip and this value can be maintained within 2.5 mK for more than 12 hours, however when no optical access is provided, thus with only 3K background radiation.

3.2. Development and modifications

A new vacuum chamber has been designed to allow for the optical measurements. The vacuum chamber has been machined out in a solid aluminium block chamber with 25 mm thick walls to provide a sufficient rigidity (STIM, Cachan, France) and is equipped with a Pfeiffer (Wetzlar, Germany) 300 l/s magnetic bearing turbopump directly connected to the chamber bottom plate to

minimize vibration to the system. It allows for 10^{-6} mbar vacuum base pressure before cooling down. Once cold, cryopumping on the setup upper, apparent metal parts reduces the base pressure to less than 10^{-7} mbar. The two original thermal shields, respectively connected to the 60 K and 3 K stages have been entirely redesigned to integrate optical cold stops and reflecting low-pass IR filters. The radiation shields are made of 2 mm thick aluminium sheet. These have been polished and also contain optically baffled, removable flanges to access the cold tip for sample insertion and exchange. These elements are represented on Figure 1.

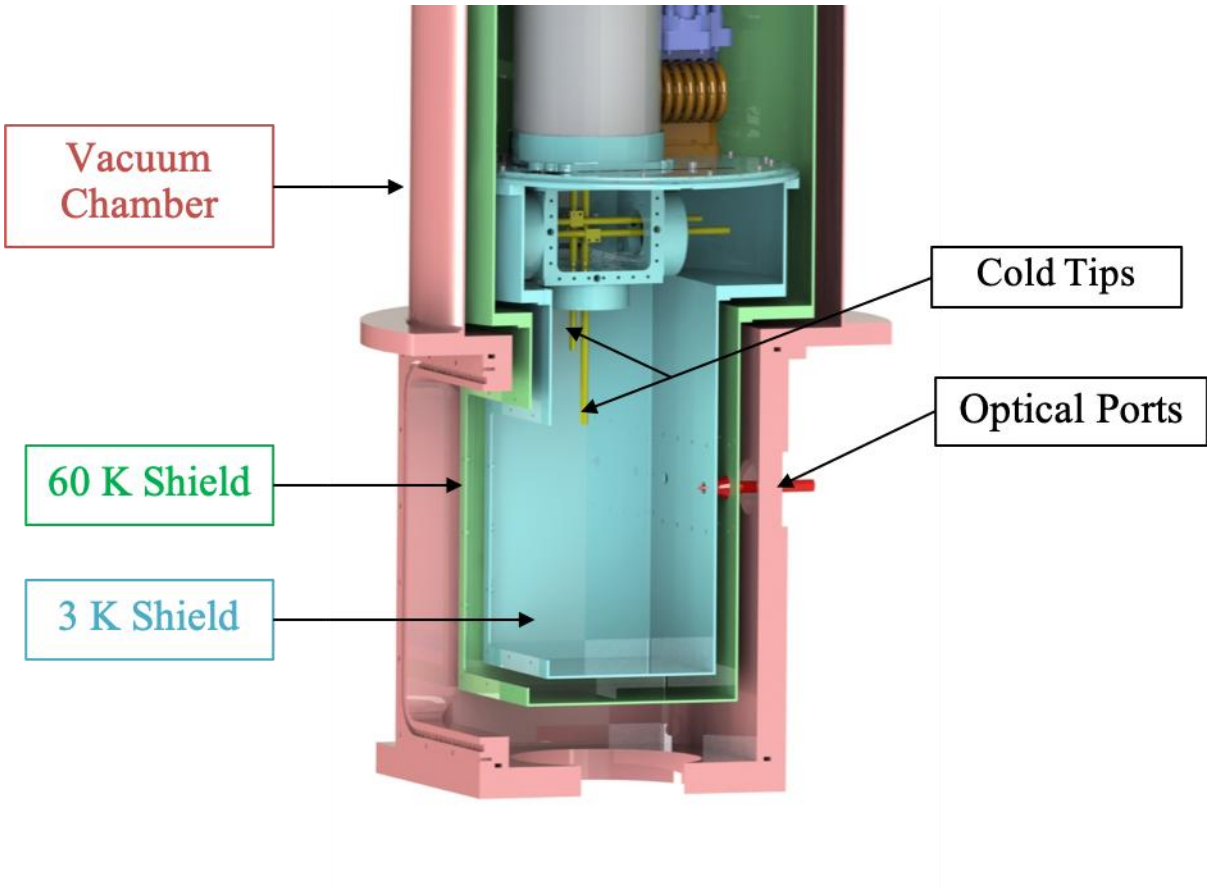

Figure 1 Viewcut of the vacuum chamber and optical shields. The main elements are identified with different colors. The 60 K stage is represented in green and the 3 K stage in light blue.

When performing spectroscopic absorption or reflection measurements of small, millimeter-size samples in cryogenic systems, it is particularly important to have a stable sample positioning with respect to the probing beam. We measured the thermal contraction of the cold tip and found that it contracts by about 1.20 mm between room and sub-K temperature. To the precision of our measurement (0.05 mm), cold tip and 3K stages follow the same displacements. To reach lower and longer-lasting temperatures, we have implemented a 500 mK stage to limit the heat load on the sample holder stage. It is clear that the low parts of the so-called 3K radiation shield are warmer than their upper attachment (up to 13 K at the bottom of the shield, 9 K at the filter level) which leads to higher IR background. Namely, we estimated the heat load on the sample stage from a 3K

surrounding to ≈1 µW, while, with the surrounding optics cooled to 500 mK intercepting half the solid angle of emission, this heat load can be reduced to about 500 nW, and even less if a third radiation shield would be added.

We thus developed an additional lower temperature plate, rigidly fixed to the 3K stage with rods made of AXM-5Q POCO graphite from EDM (one of the best insulator at sub-Kelvin temperatures [9]), to serve as a base for the optics which would follow the thermal contractions and thus keep the same alignment with respect to the cold tip. A cold optical condenser is then placed on this stage. To minimize further the radiation heat load of these metal parts lying very close to the sample holder attached to the coldest tip, the cold optics plate is thermally anchored to the 500 mK tip. This 500 mK stage is in thermal contact with the GGG rod (see Figure 2) while the sample holder is thermally connected to the coldest point, the FAA rod. The thermal conduction is carried out through six, 20mm-wide sheets of Oxygen-Free Electronic copper (C10100), an efficient conductor at low temperature [10]. With optics and sample holders both cooled to almost the same temperature, it is possible to readjust easily the optical alignment by slightly re-steering the beam from the outside and this can be checked by visual inspection of the centering of the focus point on the "3K" aperture stop and THz filter (figures 2 to 4).

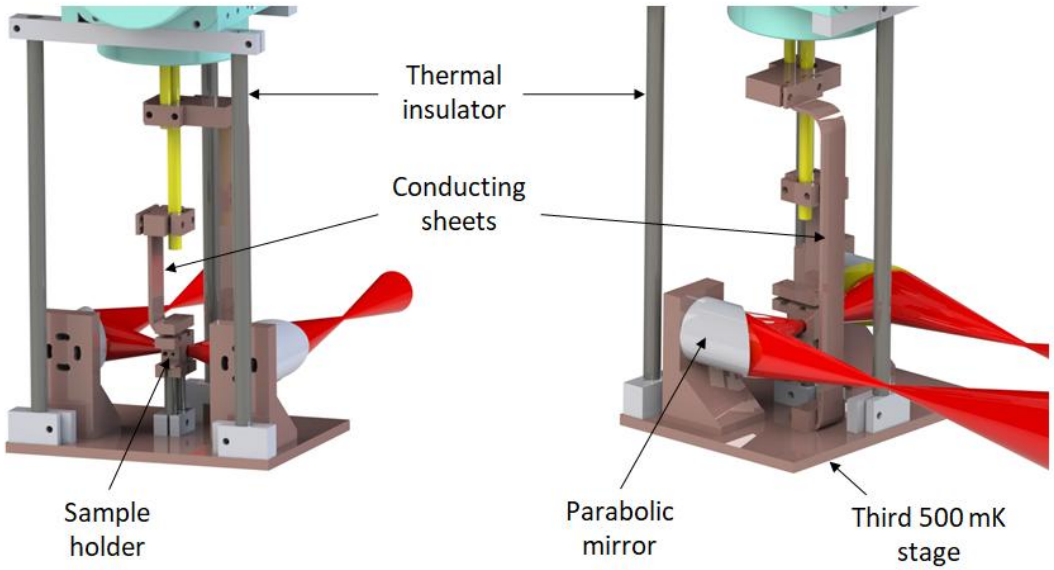

Figure 2 Back (left) and front (right) view of the cold optical system and sample holder. The third, 500 mK stage is fixed to the second, 3 K stage with thermal insulator rods. This latter stage and the sample holder are cooled down thanks to thermal conducting OFHC Cu sheets connected to the GGG and FAA rods, respectively. Two cold parabolic mirrors allow the focalisation and collection of the beam (in red: the FIR beam).

4. Optical system

Cold optics. Our requirement imposes at most a 2 mm diameter focus spot at the sample position. In order to minimize the SR beam power loss while keeping the background radiation to a low level, we chose an optical configuration with a beam secondary focus point at the entrance of the 3K shield and a cold condenser optical system consisting of two elliptical, gold-coated copper mirrors with 1:2 magnification for condensing and 2:1 magnification for collection (figure 3).The maximum size of the aperture stops on the 3K shield are thus 4 mm.

The temperatures of 50 mK for the sample holder and 500 mK for the cold optics stage were only obtained when the system was optically hermetic. For spectroscopic studies, however, optical apertures are required in the consecutive radiation shields for the introduction of the IR and/or THz beam, which, in turn, degrade strongly the minimal temperature attainable on the sample. In order to compromise between minimizing heat load and maximizing the useful photon flux, the spectral range and the size of the iris apertures at the entry and at the exit of the cryostat can be changed. The aperture size is selected using two aperture stops and the spectral range is chosen with different reflecting metal mesh filters (QMC, Cardiff, UK). The optical path of the beam is illustrated in the Figures 2 and 3, with focal points in the plane of the 3K shield. Alignment only requires focussing the light beam on the axis of the aperture stop, which can be conveniently done using the visible part of the SR beam prior to the measurements.

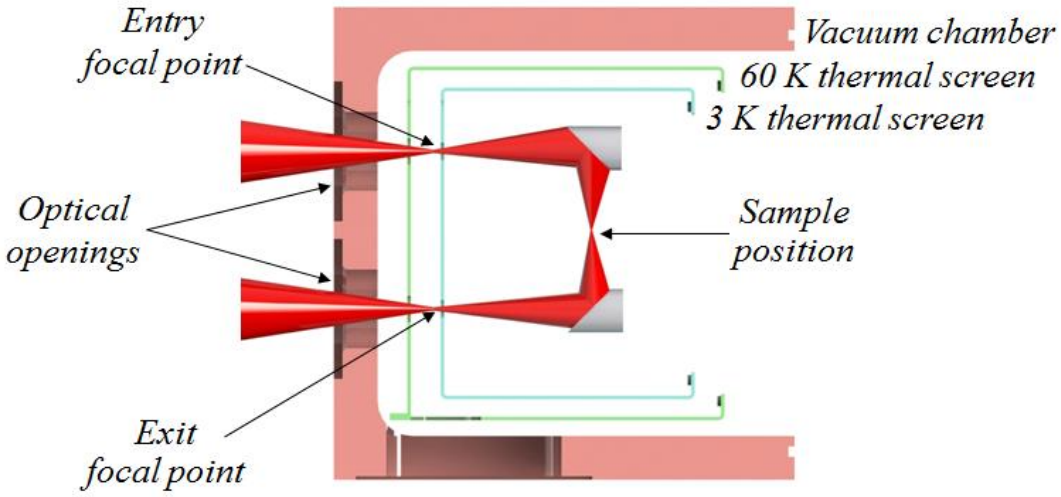

Figure 3 View-cut representation of the optical path of the beam to the sample. The beam enters the vacuum chamber through large optical openings but passes through the "3K" thermal shield at two focal points (entry and exit) in order to limit the background radiation reaching the interior of the cryostat. Another focal point is located at the sample position between the two 0.5K elliptical mirrors.

4.1. Room temperature optics

An intermediate compartment is inserted between the interferometer and the cryostat and contains the optics dedicated to transporting the modulated beam. This compartment is isolated by IR-transparent

polycrystalline diamond 19 mm diameter windows (Applied Diamond, Wilmington, USA), so that it can be vented to atmosphere even while the cryostat is operating. Inside this compartment, an adjustable periscope consisting of two pairs of mirrors at 45° incidence is placed in front of the entrance and exit apertures of the cryostat, the second pair is supported by a motorized vertical translation stage (perpendicular to the plane of figure 4). It allows controlling the height of the beam, while maintaining its orientation. This control is used during measurements to compensate the thermal contraction of the optical elements inside the cryostat when the temperature decreases. The top two periscope mirrors allow for refocusing the beam on the entrance of the refrigerator chamber.

Depending on the material under study (metals, semi-conductor or insulator), transmission or reflectivity measurements are required. In some cases, these two modes can be combined giving complementary information. With this ensemble, both optical configurations are available and can be selected under vacuum with motorised flip mirrors or right-angle mirror. They are represented in the Figure 4.

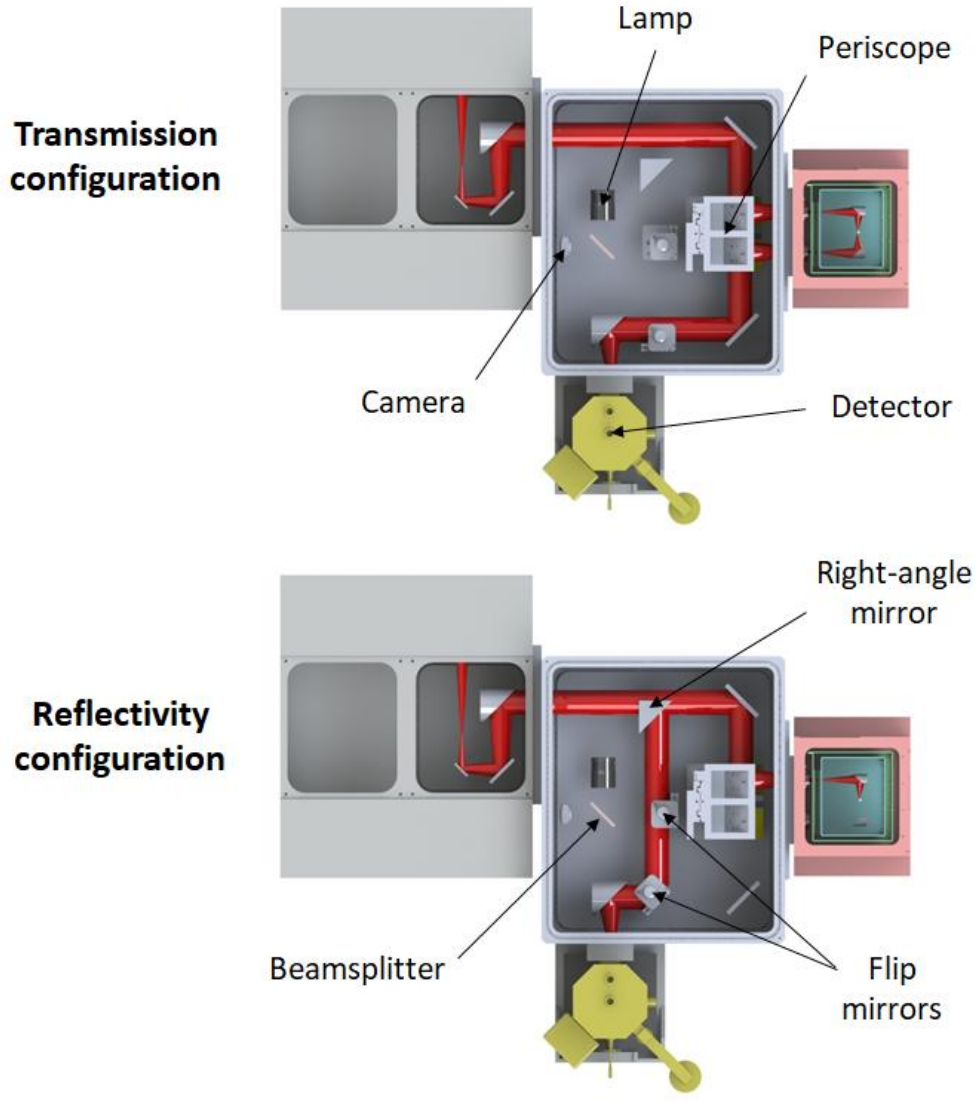

Figure 4 Transmission (top) and reflectivity (bottom) optical configurations of the setup. The periscope allows the beam to enter in the cryostat and then, after the interaction with the sample, to reach the detector. The change between transmission and reflectivity is possible with a right-angle, dividing mirror and two flip mirrors. The camera, lamp and additional beamsplitter are used for the alignment of the beam on the entrance aperture stop.

For transmission measurements, the entire modulated output beam of the interferometer goes to the periscope, which focuses the beam on the first iris. After transmission through the sample by both cold mirrors, the beam follows a symmetrical path towards the exit iris and back to the detector through the other side of the periscope.

For reflectivity measurement, half of the interferometer collimated output beam is cut using a right-angle mirror and only half the radiation reaches the sample following the same optical path as for the transmission configuration. Only half of the first, cold parabolic mirror is used at this point. After the reflection on the sample, the light is collected by the other half of the same parabolic mirror and redirected on the same entrance iris stop and, next, on the reflective face of the right-angle mirror, to be sent to the detector.

A third configuration allows for the alignment of the beam spot onto the sample. The optical path is the same than for the reflectivity measurement, except that the beam is not sent to the detector but to a camera. A white lamp and a beamsplitter illuminate the surrounding elements and the visible part of the SR beam can be used to correctly focus the beam on the aperture. The combination of the camera and the periscope is essential to maintain the alignment through the thermal contraction of the system.

5. Tests and performances

5.1. Cryogenics

The minimal temperature at the sample holder depends mostly of two experimental conditions, i.e. the size and numbers of the optical aperture stops and the spectral range of the filters placed immediately behind. The choice for these parameters is adapted in function of the spectroscopic study: the material, the energy of the excitation and the expected temperature. If the measurements require a temperature less than 100 mK, the diameter of the openings must be reduced to less than 3 mm to reduce the heat load of the background emission. However, the alignment of the system becomes more critical and the signal somewhat less intense (depending of the spectral range [8]).

It is clear from the description of the optical setup in the preceding section that, in the transmission configuration, two optical ports are needed, but only one in the reflectivity configuration. Thus for measurements limited to reflectivity, one optical port can be blocked and the background thermal load will be half that in the transmission mode, allowing for colder temperatures.

The same conclusion can be drawn for the spectral range. For the THz domain (defined here as 10 to 100 cm^{-1}), the background power reaching the sample is low and the cryogenic performances are

optimal. When it is necessary to increase the spectral domain investigated, for example in the FIR domain (10 to 600 cm^{-1}), the lowest reachable temperature at the sample increases significantly.

As explained above, an ADR cryogenerator has a cyclic operation and, in presence of continuous (conduction, radiative) heat loads and in absence of continuous cooling power, no constant "measurement temperature" can be maintained. Rather it is more realistic and useful to define a "hold time" during which a *given maximum temperature drift* can be guaranteed, starting from a *given, low temperature*. Of course, for spectroscopy, this hold time must be long enough to perform the required measurements with the desired signal-to-noise (S/N) ratio. This is where the use of SR is here essential, as it has been shown elsewhere that, when using small-size samples or high resolution, the small effective size and high brightness of the source offers a major advantage [8, 11]. Past experiences have shown that such measurements with a given, acceptable S/N are obtained within an hour when days are typically needed with conventional black body sources. Also, to obtain usable, physically meaningful data the temperature drift must remain small during data acquisition. We thus rather arbitrarily define our hold time as *the time during which data can be collected within a temperature drift of 2.5mK*, half the absolute accuracy of our temperature sensing system.

Needless to say, hold times notably less than 10 minutes are of limited practical use. On figure 5, we present the temperature drift measured during a reflectivity measurement on a thin film STO sample, using a 2 mm aperture diameter for 10 - 100 cm^{-1} spectral range (middle, red curve). This can be compared to a measurement taken in identical conditions, but without the probing SR beam (lower, black curve). In this configuration, the lowest temperature obtained *without* probe beam is about 95 mK and *with* probe beam, it jumps (around time 30 mn) to 99 mK. The corresponding hold times are here about 190 min without probing beam and 120 minutes with beam. The upper, green curve corresponds to the exact same conditions, but with the two optical apertures needed for a transmission measurement. The lowest temperature reached is then 144 mK and the hold time is reduced to 97 minutes.

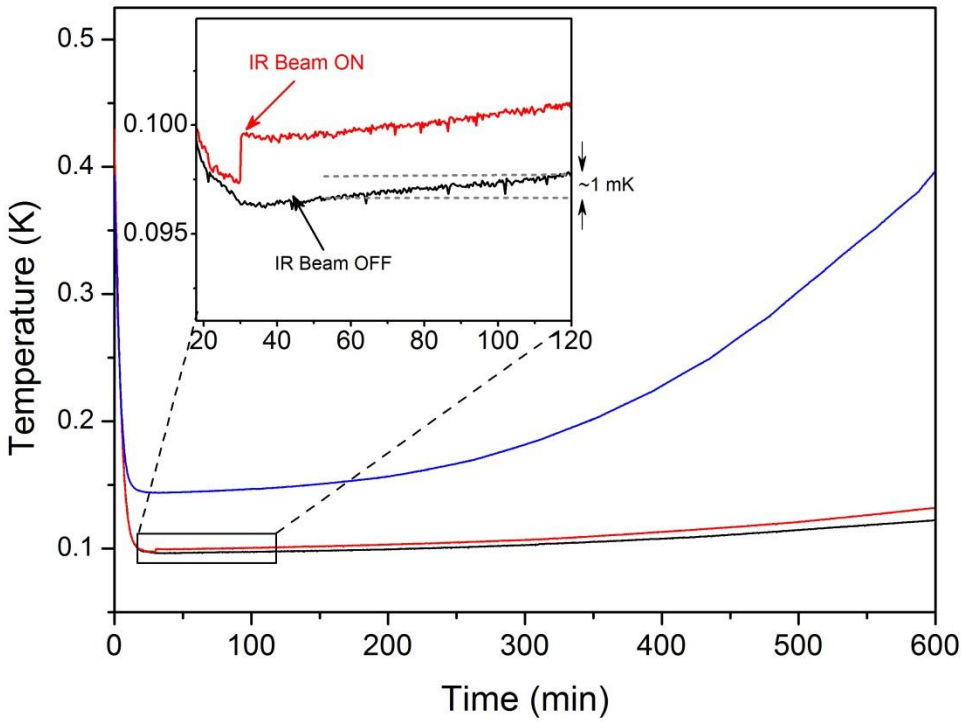

Figure 5 Temperature vs time for a reflectivity measurement. The cold aperture diameter is 2 mm, the sample diameter is 1mm, spectral range 10 - 100 cm^{-1}. Lower curve (black): no beam, middle curve (red) with beam from time = 30 mn. Upper curve (blue) same measurements but two optical ports for transmission spectra. Time zero corresponds to the end of the magnetic cycle.

From these data, using the charts provided by HPD with heat capacities and conductivities of their system, it is relatively straightforward to derive the power of the incoming background radiation and conduction losses (≈600 nW) and of the absorbed part of the SR beam in this range (40 nW). The latter can be compared to the power estimated at the spectrometer output in the same range (70 nW). Given the system losses (filters (10%) and windows (25%) transmission losses, etc…), we can consider these values in reasonable agreement.

5.2. Transmission measurements

The data presented in figure 6 have been obtained in approximatively 10 minutes of measurement in either the THz or the FIR domains. The source is the synchrotron radiation and the optical configuration is in transmission.

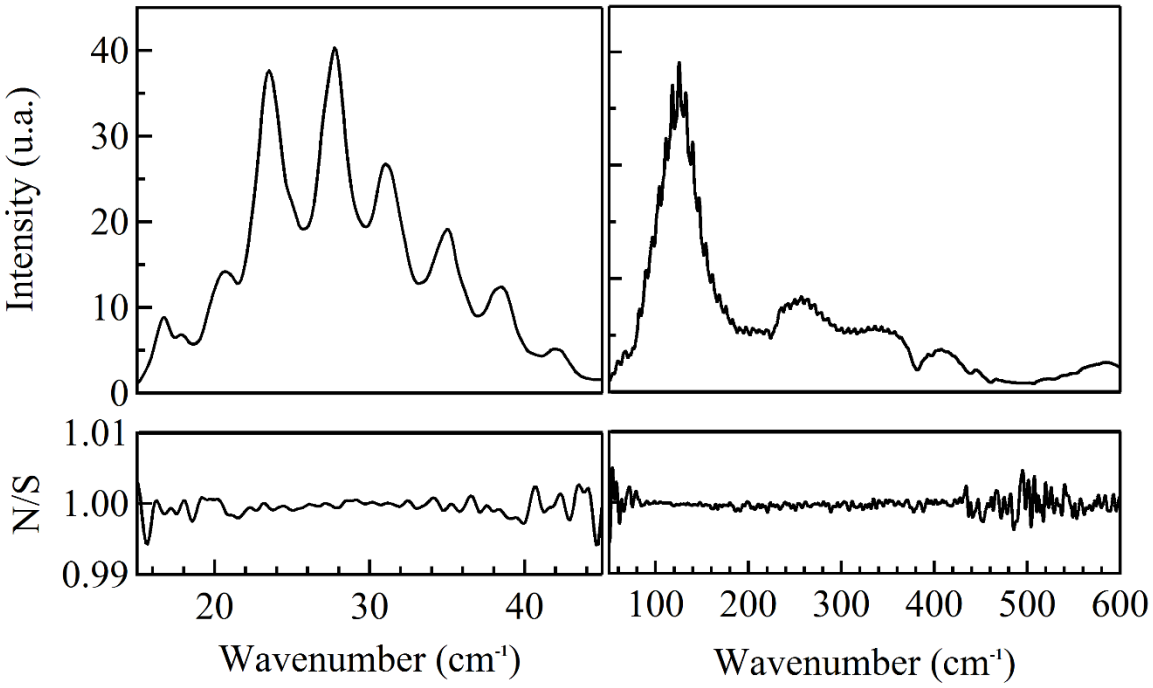

Figure 6 Intensity of the signal (top) and corresponding noise-to-signal ratio (bottom) of the reference test for the THz (left) and FIR (right) spectral domains, obtained in 5 min for a spectral resolution of 0.5 cm^{-1}.

For the THz domain, the noise-to-signal ratio is less than 1 % over the spectral range 10 – 50 cm^{-1}, and reaches 0.1% between 15 cm^{-1} and 45 cm^{-1} at 0.5 cm^{-1} resolution. This value can be slightly improved by increasing the acquisition time. The high and low frequency limits are limited by the beamsplitter of the Michelson interferometer, here a 50 µm Mylar. The detection is performed with a bolometer held at 1.6 K by pumping on the liquid helium.

For the FIR range, this ensemble allows to cover a wide range ranging from 50 to 600 cm^{-1}. Between 80 and 450 cm^{-1}, the signal-to-noise ratio is optimal with a value of 1000 peak-to-peak. It becomes about 100 below 80 cm^{-1} and over 450 cm^{-1}. The low and high frequency limits are respectively caused by the beamsplitter, a 6 µm Si-coated Mylar, and the detector, a 4 K helium-cooled bolometer.

6. An example: THz study of Nb thin films superconducting gap

In order to illustrate the scientific capabilities of this ensemble, the spectroscopic study of a 4 nm thick niobium film is presented thereafter. This sample has been grown using an electron gun evaporation technique on a 300 µm thick sapphire substrate and superconductivity has been evidenced with a critical temperature of 6.3 K [12].

By means of optical spectroscopy, the superconducting gap feature of Nb can be investigated as a function of temperature, which provides significant information on the nature of the mechanism at the origin of superconductivity. In Nb bulk for example, the energy gap at very low temperature, namely

$2\Delta_0$, is about 24 cm^{-1} in the THz range [13]. Therefore, the spectroscopic setup described previously is well-adapted to this scientific case, as it allows to probe the superconducting gap at $T \ll T_C / 10$, where the corresponding feature is the most intense and located at a maximal energy $2\Delta_0$.

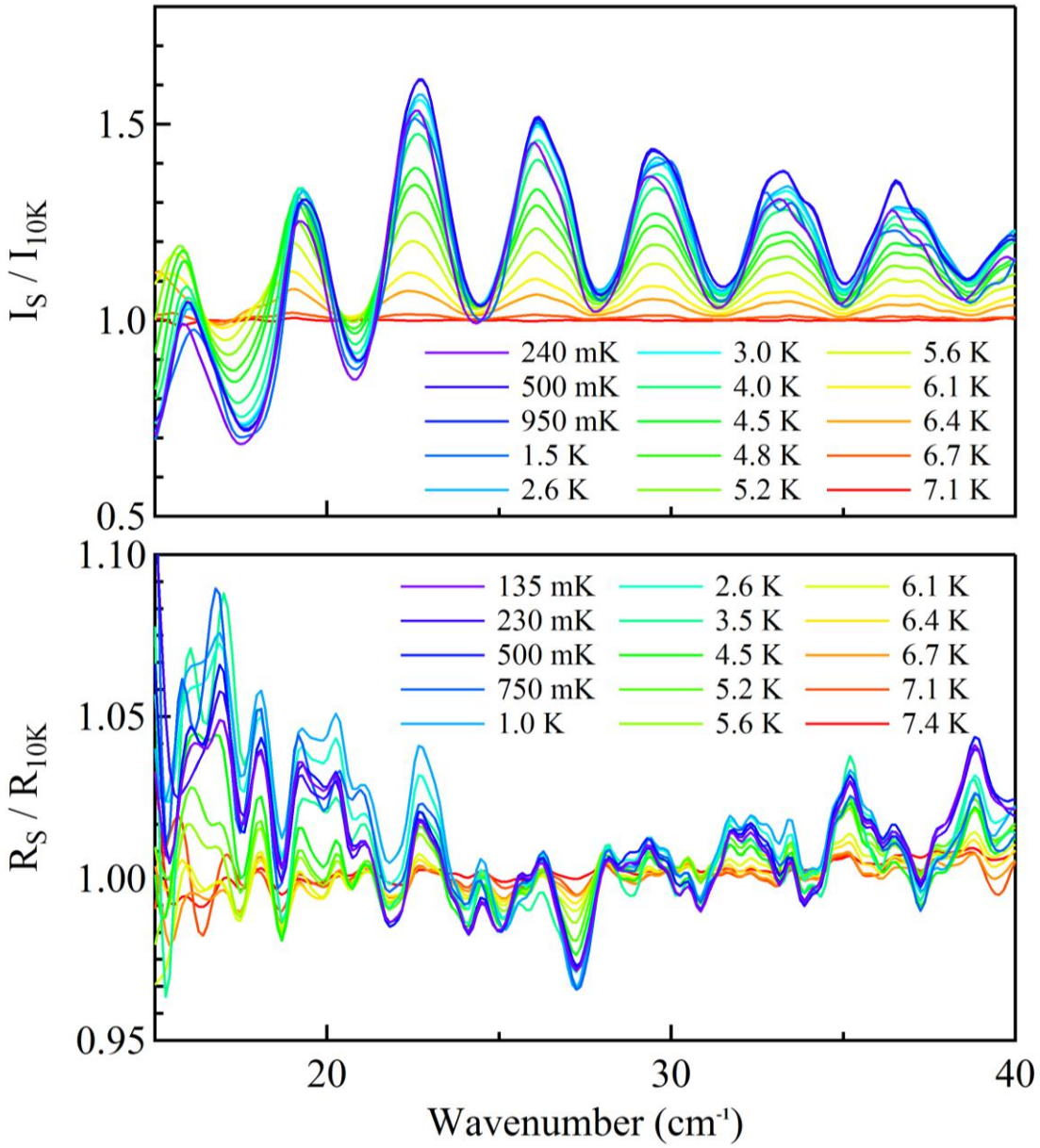

Figure 7 Temperature relative ratios of transmission (top) and reflectivity (bottom) for the 4 nm Nb thin films in the THz range. The reference is the signal of the sample in the normal state at 10 K.

The Figure 7 shows the spectroscopic measurements performed in the THz range with the new ensemble. Data are exposed as temperature relative ratios of transmission (I_S/I_{10K}) and reflectivity (R_S/R_{10K}), where I_S and R_S are the signals in the superconducting state and I_{10K} and R_{10K} in the normal metallic state at 10 K. The strong channeling features are due to internal reflections within the

sapphire substrate slab and their changes with temperature when the Nb film reaches a supraconducting state.

For both optical configurations, the superconducting gap of Nb is evidenced. At the minimal temperature, here 135 mK for reflectivity and 240 mK for transmission, the maximal gap energy $2\Delta_0$ is observed around 19 cm^{-1}. When increasing the temperature, the intensity of the feature decreases accordingly and its energy shifts towards low energy, as predicted by the conventional BCS theory [14]. Data treatment will be detailed in a future paper, but these results demonstrate that the new spectroscopic setup allows observing small intensity excitations in the THz and the FIR spectral ranges.

7. Conclusions

In conclusion, we described here an ensemble dedicated to the THz and IR spectroscopies at sub-Kelvin temperatures, available on the AILES beamline of synchrotron SOLEIL. This instrument is suited to investigate quantum effects occurring in condensed matter, as demonstrated by the study of the superconducting gap within a Nb thin film. Thanks to the synchrotron radiation, measurements can be performed in transmission and in reflectivity with an excellent reproducibility at temperatures lower than 200 mK.

Acknowledgements

The authors thank Charlie Manaher (HPD) and C. Poulalion (STIM, France) for useful discussions and help in the system design. The authors acknowledge funding from ANR Dymage ANR-13-BS04-0013-01. We are grateful V. Bouchiat (Institut Neel, Grenoble, France) for providing the samples.

References

[1] W.J. Padilla, Z.Q. Li, K.S. Burch, Y.S. Lee, K.J. Mikolaitis, D.N. Basov, Rev. Sci. Inst. 75(11) (2004) 4710.

[2] N. Maleeva, L. Grünhaupt, T. Klein, F. Levy-Bertrand, O. Dupré, M. Calvo, F. Valenti, P. Winkel, F. Friedrich, W. Wernsdorfer, A. V. Ustinov, H. Rotzinger, A. Monfardini, M. V. Fistul, I. M. Pop, Nature Comm. 9 (2018) 3889.

[3] Row et al. Rev. Sci. Inst. 87 (2016) 033105.

[4] G.M. Klemencic, P.A. Ade, S. Chase, R. Sudiwala, A.L. Woodcraft, (2016) Rev. Sci. Inst. 87, 045107.

[5] S. Hähnle, J. Bueno, R. Huiting, S.J. Yates, C., Baselmans (2018) J. Low Temp. Phys. DOI.org/10.1007/s10909-018-1940-1.

[6] H. McCarrick, et al. Astronomy & Astrophysics 610 (2018) A45.

[7] E.R. Switzer, P.AR. Ade, T. Baildon, D.Benford et al. Rev. Sci. Inst. 90 (2019) 095108649.

[8] P. Roy, M. Rouzières, Z. Qi, O. Chubar. *Infrared Physics & Technology*, **49** (2006)139-146.

[9] Woodcraft, A.L. & Gray, A. *AIP Conference Proceedings*, **1185** (2009) 681.

[10] Woodcraft, A.L. *Cryogenics*, **45** (2005) 626-636.

[11] A. R. W. McKellar, J. Mol. Spectrosc. **262** (2010) 1.

[12] C. Delacour, L. Ortega, M. Faucher, T. Crozes, T. Fournier, B. Pannetier, V. Bouchiat, *Physical Review B*, **83** (2011) 144504.

[13] V. Novotny, P.P.M. Meincke, *Journal of Low Temperature Physics*, **18** (1975)147 - 157.

[14] Bardeen, J., Cooper, L.N. & Schrieffer, J.R. (1957). *Physical Review*, **108**, 1175 - 1204.